NASA Technical Paper 1941

December 1981

Laboratory Measurements of Physical, Chemical, and Optical Characteristics of Lake Chicot Sediment Waters

William G. Witte,
Charles H. Whitlock,
J. W. Usry,
W. Douglas Morris,
and E. A. Gurganus

NASA

NASA
Technical
Paper
1941

1981

Laboratory Measurements of Physical, Chemical, and Optical Characteristics of Lake Chicot Sediment Waters

William G. Witte,
Charles H. Whitlock,
J. W. Usry,
W. Douglas Morris,
and E. A. Gurganus
Langley Research Center
Hampton, Virginia

NASA
National Aeronautics
and Space Administration

**Scientific and Technical
Information Branch**

SUMMARY

Reflectance, chromaticity, diffuse attenuation, beam attenuation, and several other physical and chemical properties are measured for various water mixtures of bottom sediment from Lake Chicot, Arkansas. Mixture concentrations range from 5 ppm to 700 ppm by weight of total suspended solids in filtered deionized tap water. Upwelled reflectance is observed to be a nonlinear function of total suspended solids with the degree of nonlinearity a strong function of remote-sensing wavelength. Near-infrared wavelengths appear useful for monitoring highly turbid waters with sediment concentrations above 100 ppm. Chromaticity characteristics do not appear useful for monitoring sediment concentrations above 100 ppm. At both visible and near-infrared wavelengths, beam attenuation correlates well with total suspended solids ranging over two orders of magnitude.

INTRODUCTION

The feasiblity of applying remote-sensing technology to agricultural programs was initially established during a 4-year investigation conducted by the United States Department of Agriculture (USDA); more than 2000 potential uses were documented. Consequently, five federal agencies, including the USDA and the National Aeronautics and Space Administration (NASA), have entered into a 6-year joint program called AgRISTARS (Agriculture and Resources Inventory Surveys Through Aerospace Remote-Sensing). This program's objectives are to develop the technology and test the capability of economically employing remote sensing in several areas such as crop inventory, conservation, water resources management, and snowpack assessment.

Federal legislation requires that the USDA monitor and report pollution levels and their effects. To meet this requirement, the assessment of various conservation practices may be performed by analyses of remotely sensed data.

Sediment is the primary water pollutant of concern in assessing conservation practices. Remote-sensing methods are needed to measure and monitor this pollutant for concentrations up to 1000 ppm. These remote-sensing data are necessary for input to pollution models. During fiscal year 1980, two sites were selected for USDA/NASA pilot field studies, and initial laboratory tests were performed to define physical, chemical, and optical characteristics of the particular sediment waters. One of these sites was Lake Chicot (fig. 1), an oxbow lake located adjacent to the west bank levee of the Mississippi River in Chicot County, Arkansas. Lake Chicot is an old cutoff channel of the Mississippi River and is the largest lake in Arkansas.

Field studies of Lake Chicot were conducted throughout 1980 by the USDA. On two occasions, in March and December, samples of Lake Chicot bottom sediment were sent for tests to the Marine Upwelled Spectral Signature Laboratory (MUSSL) at the Langley Research Center.

In the laboratory, remote-sensing reflectances, attenuation coefficients, and other physical and chemical properties were measured over a wide range of sediment concentrations. Upwelled reflectance was measured for wavelengths between 400 and 980 nm and the relationship between attenuation and concentration was examined at selected wavelengths. In addition, chromaticity characteristics for the mixture

concentrations were calculated. It is the purpose of this paper to present and discuss these data and to point out their usefulness in monitoring sediment concentrations for input to pollution models.

SYMBOLS

A	area of spectrometer entrance slit, cm^2
C	white light chromaticity
c	beam attenuation coefficient, m^{-1}
D	vertical displacement of oscilloscope measurement, cm
$E(\lambda)$	spectral irradiance, $\frac{W}{m^2\text{-}nm}$
E_D	downwelled irradiance, $\frac{W}{m^2\text{-}nm}$
K	ratio of instrument throughput $A\Omega$ to vertical-scale sensitivity factor S, $\frac{cm^2\text{-}sr}{mW/nm\text{-}cm}$
K_{bb}	diffuse attenuation coefficient obtained from broad-band meter, m^{-1}
K_{nb}	diffuse attenuation coefficient obtained from narrow-band photometer, m^{-1}
$L_u(\lambda)$	upwelled spectral radiance, $\frac{mW/nm}{cm^2\text{-}sr}$
$L_{so}(\lambda)$	upwelled radiance above water surface from 99-percent near-Lambertian reflector, $\frac{mW/nm}{cm^2\text{-}sr}$
$P(\lambda)$	spectral power, mW/nm
S	vertical-scale sensitivity factor, mW/cm-nm
s	depth in water, m
x,y	chromaticity coordinates
λ	wavelength, nm
$\rho_u(\lambda)$	spectral reflectance (relative to a 99-percent (near-Lambertian) reflector), percent of input
σ	standard deviation of instrument error
Ω	acceptance solid angle of spectrometer, sr

EXPERIMENTAL PROCEDURE

Laboratory tests were conducted within the arrangement shown in figure 2. Major parts of the system include a water tank, circulation system, filtration and deionization system, solar simulator, first-surface mirror, and rapid-scan spectrometer. The light source is a 2.5-kW xenon short-arc lamp which produces a spectrum similar to that of the Sun (ref. 1) with about 50 percent of its sea-level intensity. This system is the same as that used in tests reported in reference 2. Figure 3 shows standard sea-level solar irradiance spectra and the solar simulator spectrum, normalized to the irradiance at λ = 600 nm, compared with the normalized irradiance curve for a solar elevation angle of 30°. A more complete description of the laboratory equipment is given in the appendix.

Two samples of Lake Chicot bottom sediments were tested, one in March 1980 and the other in December 1980. The water tank was filled to within 0.3 m of the top with 11 600 liters of conditioned tap water (filtered and deionized). Just prior to testing, the sediments (which had been shipped in several containers) were combined in a large vat and stirred. This procedure ensured homogeneity among subsequent samples or increments. Small amounts of sediment were withdrawn from the vat, put into a graduated cylinder, and then gradually added to the water tank until the transmission of the mixture in the tank was approximately 65 percent, which corresponds to a beam attenuation coefficient of 5 m^{-1}. The transmission was measured with a modified Model 912S Hydro Products Transmissometer with a beam path length of 10 cm and a filter with a peak transmission of 560 nm and half-maximum band-pass width of 80 nm. (Reflectance of the clear water was not measured because reflectance of light from the tank bottom might influence the upwelled signal.) The quantity of sediment added was noted. Estimates were made of the increments needed to obtain a range of sediment concentrations in the water tank covering the concentration range (5 ppm to 700 ppm) likely to be observed at Lake Chicot.

The circulation system was activated and the mixtures were circulated without filtration. At the start of the experiment a radiance spectrum was measured of light reflected from a plate painted with a 99-percent reflective paint (white card) placed near the surface of the water. The same measurements were made halfway through and at the end of the experiment to check for instrument drift. Also, these data were used with the radiance spectra for the various sediment concentrations to obtain corresponding reflectance spectra. The circulation system remained on for the duration of the experiment.

After the white card measurements, an upwelled radiance spectrum for the first concentration was obtained. Then the next increment of Lake Chicot sediment was mixed with the water in the tank to achieve the second concentration. This mixture was allowed to circulate for approximately 15 minutes until the sediment was evenly distributed throughout the tank. An upwelled radiance spectrum was measured as before. The procedure was repeated to obtain upwelled spectra for all concentrations tested.

For the December test only, after the upwelled radiance spectrum for each concentration was obtained, downwelled irradiance through the mixture was measured at depth intervals down to the 1-percent photic zone depth of the mixture. Two irradiance meters, a Kahlsico radiometric submarine photometer Model 268WA390, and a LI-COR quantum meter Model LI-185A with a LI-COR quantum sensor Model 192S were used. The Kahlsico instrument measured downwelled irradiance in three wavelength bands, the blue (430 to 490 nm), the green (490 to 570 nm), and the red (620 to 680 nm). The quantum instrument measured downwelled irradiance across the visible wavelength range

(from 400 to 700 nm). For each concentration, downwelled irradiance E_D was plotted on semilogarithmic paper as a function of depth s. A straight line was faired through the points and a diffuse attenuation coefficient, K_{nb} or K_{bb}, was computed from the equation

$$K_{nb} \text{ or } K_{bb} = \frac{\ln\left(E_D / E_{D_1}\right)}{-\Delta s} \tag{1}$$

where E_D was measured at some depth and E_{D_1} was measured near the water surface.

Samples of the conditioned tap water and of each mixture were analyzed for selected physical and chemical properties, and the results are presented in table I for the March test and in table II for the December test. Total suspended solids (TSS) were obtained by the standard crucible method for both experiments and by the membrane filter method for the December test. Fiberglass filters with variable 1.2 to 1.6 μm pore size were used for the crucible method. Fiberglass filters enable volatile and nonvolatile solids, and TSS, to be measured from the same sample. The membrane filters, which are generally used in oceanographic work, have a pore size of 0.4 μm. Since they remove particles down to 0.4 μm in size, TSS obtained by this method are usually higher than those obtained by the crucible method. The TSS obtained by the crucible method are presented in the figures and discussed in the text of this report.

For the December experiment other samples were used in a prototype small angle scattering meter (ref. 3) to measure beam attenuation coefficients c at wavelengths of 550 nm and 750 nm for each concentration. This instrument has various path lengths and a small acceptance angle (less than 0.1°) so that forward scattering contributions are negligible (less than 10 percent) in the range $0.1\ m^{-1} \leqslant c \leqslant 325\ m^{-1}$. The beam attenuation data are presented in table II.

RESULTS AND DISCUSSION

Reflectance

Measured spectral radiance curves are shown in figure 4 for the 99-percent (near-Lambertian) white card and in figure 5 for the water mixtures of the March and December tests. Spectral reflectance curves, as a ratio of the water mixture radiance to white card radiance, are shown in figure 6 for the two tests. Both radiance and reflectance generally increase at all wavelengths with increasing concentration of suspended solids. Reflectance curves for the two experiments have approximately the same characteristics. The peak reflectance occurs at about 580 nm for the lower concentrations and gradually shifts to about 740 nm for the highest concentration. As sediment concentration was increased from approximately 5 ppm, a condition was reached where sediment increases had less and less effect on reflectance first at the blue, later at the green, and finally at the red wavelengths. This effect is shown graphically in figure 7 which presents $\rho_u(\lambda)$ as a function of TSS at selected wavelengths. At low concentrations, $\rho_u(\lambda)$ increases sharply at 450, 550, and 650 nm; but at concentrations of roughly 100, 200, and 300 ppm, respectively, the $\rho_u(\lambda)$ curves become nearly asymptotic, i.e., saturated. At near-infrared wavelengths of 750, 840, and 900 nm, the curves have less slope than those in the visible region at low sediment concentrations but continue to increase for TSS values as high as 700 ppm. These results are consistent with the simplified model

calculations of reference 4 and with satellite field data in references 5 and 6. Upwelled reflectance from the water column is not a linear function of TSS except over limited concentration ranges. The degree of nonlinearity is a function of wavelength.

Chromaticity

Optical chromaticity of upwelled radiance spectra has received attention as one property which may be useful for remote monitoring of suspended sediments (ref. 7). For this reason, chromaticity characteristics were calculated for each of the reflectance spectra shown in figure 6 using the International Commission on Illumination (ICI) standard functions (see ref. 8). Results of these calculations are shown in figure 8. Point C represents the coordinates of ICI Illuminant C on which most color observations are based. A straight line from point C through a water mixture point extended to the locus line of color gives the dominant wavelength of that water mixture. That process applied to each water mixture point indicates that dominant mixture color ranged from 560 nm for low sediment concentrations to 583 nm for the highest turbidities. These changes in dominant color do not agree with the observed shift to a maximum of 740 nm shown in figure 6. Large changes in chromaticity coordinates x and y occurred when concentration varied from 5 ppm to 100 ppm, but only small changes were evident from 100 ppm to 700 ppm. These controlled-experiment data confirm similar observations from a simplified theoretical model (ref. 7) and from field measurements with multiconstituent waters (ref. 9). Similar results from all of these sources indicate that chromaticity characteristics may not be useful for quantifying concentrations in waters with large amounts of sediment.

Diffuse Attenuation

The diffuse attenuation coefficient (sometimes known as the extinction coefficient) is often used as an important parameter for estimating primary productivity of marine life. It is desirable to relate diffuse attenuation coefficient at various wavelengths to values of sediment concentration. It is also desirable to relate wavelength-dependent diffuse attenuation coefficients to broad-band visible wavelengths which are often obtained by low-cost field instruments. As mentioned previously, underwater downwelled irradiance measurements were made with a three-band photometer and a broad-band meter during the December tests. Figure 9(a) shows diffuse attenuation coefficients (K_{nb}) obtained with the narrow-band instrument, and figure 9(b) presents diffuse attenuation coefficients (K_{bb}) obtained with the broad-band instrument. Comparison of K_{bb} with K_{nb} for similar sediment concentrations indicates that broad-band measurements were similar to narrow-band values at green wavelengths (490 to 570 nm) in the prepared waters of the laboratory tests. It is expected that broad-band measurements in the field would also be indicative of green wavelength diffuse attenuation values if the water has high sediment concentration. At low sediment concentrations such a correlation is not to be expected, however, because optical effects of dissolved organic carbon and chlorophyll make significant contributions to the optical characteristics of the total mixture.

Beam Attenuation

An optical parameter sometimes used as an indicator of sediment concentration is the beam attenuation coefficient c, measured with an underwater transmissometer.

During the December tests, measurements of c were made with the prototype small angle scattering meter at Langley Research Center. This instrument is believed to give accurate beam attenuation measurements at high turbidities. Figure 10 shows high correlation between sediment concentration and beam attenuation coefficient over 2 orders of magnitude ($6\ m^{-1} \leq c \leq 600\ m^{-1}$) for the prepared waters of these tests. While such results make sense for single-constituent water (sediment added to filtered deionized tap water), field data should not be expected to correlate as well, particularly at low TSS values. Chlorophyll both absorbs and scatters at most visible and near-infrared wavelengths, and dissolved organic carbon absorbs at ultraviolet, blue, and green wavelengths. At high sediment concentration, however, chlorophyll and dissolved organic carbon contributions are often small in comparison to that of sediment. Correct beam attenuation measurements may then become a useful estimate of sediment concentration. The advantage of transmissometer measurements of beam attenuation coefficient is that rapid assessment of vertical concentration changes and stratification layers in the water column may be made from a boat to improve field experimental measurement procedures. An instrument carefully calibrated with sediments from the particular site is required for accurate measurements, however.

CONCLUDING REMARKS

Radiance and reflectance spectra were measured for several mixture concentrations of bottom sediment from Lake Chicot, Arkansas. Also, beam attenuation coefficients, diffuse attenuation coefficients, and several other physical and chemical parameters obtained from laboratory analyses were presented.

Based on the analyses of these data the following conclusions were drawn:

1. Upwelled reflectance from the water column is not a linear function of total suspended solids except over limited concentration ranges. The degree of nonlinearity is a function of wavelength with reflectance becoming asymptotic (or saturating) first at blue, then at green, and finally at red wavelengths as total suspended solids increase from 5 ppm to 700 ppm.

2. Although the upwelled signals in the blue, green, and red wavelength ranges saturate and become less useful for remote sensing of high concentration levels, the upwelled signals in the near-infrared wavelength range continue to respond markedly to changes in concentration over the sediment range of these tests.

3. Controlled-experiment laboratory results agree with theoretical and field data trends which indicate that chromaticity characteristics may not be useful for quantifying concentration values in waters with large amounts of sediment.

4. Broad-band meter measurements of diffuse attenuation coefficient gave values comparable to those obtained at green wavelengths between 490 nm and 570 nm in the prepared waters of these laboratory tests. Similar results are expected in field experiments if the waters have high sediment concentration with small optical contributions from chlorophyll and dissolved organic carbon.

5. In single-constituent water, beam attenuation coefficient correlates well with sediment concentration. Correct beam attenuation measurements with site-specific calibration offer the potential for rapid assessment of water column variation and concentration gradients for highly sedimented waters.

Langley Research Center
National Aeronautics and Space Administration
Hampton, VA 23665
October 6, 1981

APPENDIX

LABORATORY AND EQUIPMENT

The cylindrical, steel water tank has a 2.5-m diameter and a 3-m depth. The bottom is concave, as illustrated in figure 2. The tank interior is coated with a black phenolic paint that absorbs 97 percent of incident radiation over the spectral range of these measurements (400 to 980 nm). For these experiments, the tank was filled to within 0.3 m of the top with about 11 600 liters of water.

The circulation system was designed to maintain a vertically and horizontally homogeneous mixture in the tank and to maintain in suspension particles up to about 70 μm in diameter (specific gravity of 2.6). This particle size corresponds to fine sand. In order to accomplish these design goals, water is pumped from the drains at the bottom of the tank into a system of pipes which returns the water to the tank through two vertical pipes on opposite sides of the tank. The pipes empty just above the concave bottom. Forty-five degree couplings at the ends of the pipes direct the flow of the water counterclockwise over the concave bottom, creating a massive swirling motion of the water in the tank. Water and suspended particles generally rise near the periphery of the tank, are drawn through the vortex near the center, and return downward to the drains at the bottom. Tests using tracer techniques and transmission measurements have confirmed that this circulation system provides a near-uniform homogeneous mixture throughout the tank.

The filtration and deionization system includes a commercial fiber swimming-pool filter, an activated carbon filter, and a charged resin deionizer. These units were placed in waterlines parallel to the main circulation system waterlines and can be used separately or in any combination by using valves. The two filters remove particulates and dissolved organic materials from the water before it reaches the deionizer where dissolved ionic substances are removed. After tap water is conditioned through this system, it contains less than 0.5 ppm of suspended solids and less than 2 ppm of dissolved substances.

The light source is a solar-radiation simulator designed to approximate the spectral content of the Sun's rays. The radiation spectrum is produced by a 2.5-kW xenon short-arc lamp and is transferred to the target plane through an optical arrangement inside the simulator and a collimating lens accessory. With this lens accessory, the projected beam is collimated to a 0.15 m diameter, 0.3 m from the simulator, and has a ±2.5° divergence angle. For these experiments, the simulator was located approximately 2.0 m from the water tank as illustrated in figure 2. At this distance from the simulator, the beam is about 0.57 m in diameter. A mirror positioned 1.7 m above the water surface reflects the center of the beam to the water surface. The incidence angle with the water surface is 19° to avoid specular reflectance. The first-surface mirror is coated with aluminum and protected by an overcoat of silicon monoxide. It has a 0.3-m diameter and reflects an elliptical spot on the water surface which has a major axis of 0.35 m. The simulator spectral input to the water surface is similar to, but not a precise duplicate of, sea-level standard solar-radiation curves often used in engineering calculations (ref. 1). Figure 3(a) shows that the standard sea-level curves are quite variable, depending on the solar elevation angle. Figure 3(b) shows the simulator spectrum normalized at 600 nm compared with the normalized solar spectrum at a solar elevation angle of 30°. These curves suggest that when laboratory measurements are made at a 32-nm spectral resolution, the input spectrum and possibly the output measurements are similar to those that would be expected in the field if the solar elevation angle is on the order of

30°. The total intensity of the light hitting the water surface is approximately 50 percent of that in actual field conditions.

The rapid-scanning spectrometer system consists of a spectrometer unit with a telephoto lens attachment and a plug-in unit with an oscilloscope and camera attachment. The spectrometer unit with telephoto lens attachment is mounted 2.3 m above the surface of the water as illustrated in figure 2. The spectrometer uses a Czerny-Turner monochromator without an exit slit. The spectral output of the monochromator is focused on the target of a vidicon where the spectrum is stored as an electrical charge image. An electron beam periodically scans the vidicon target to convert the charge image into an electronic signal. This signal is processed by the plug-in unit which also functions as a controller between the spectrometer and the oscilloscope. The signal is displayed on the oscilloscope and is photographically recorded with a camera. The spectrometer is designed to measure power per spectral bandwidth (spectral power). The oscilloscope screen is used to show displacement of the instrument measurement. Oscilloscope displacement is proportional to spectral power, as shown in the equation,

$$D = \frac{P(\lambda)}{S} \tag{A1}$$

The signal is internally processed in such a manner that the vertical-scale sensitivity factor S has a constant value over the wavelength range from 400 to 980 nm. Values of S were obtained by the manufacturer using calibration procedures described in reference 10. (After receipt of the instrument, the manufacturer's calibration was checked in an approximate manner prior to the tests described herein.) The upwelled spectral radiance $L_u(\lambda)$ is defined as

$$L_u(\lambda) = \frac{P(\lambda)}{A\Omega} \tag{A2}$$

where A is the area of the spectrometer entrance slit and Ω is the acceptance solid angle of the spectrometer.

Combining equations (A1) and (A2) results in

$$L_u(\lambda) = \frac{DS}{A\Omega} \tag{A3}$$

or

$$L_u(\lambda) = \frac{D}{K} \tag{A4}$$

where

$$K = \frac{A\Omega}{S}$$

Thus, upwelled spectral radiance is determined from oscilloscope displacement and the proportionality constant K which is a function of the calibration factor S (which includes optical transmissivity) as well as acceptance angle Ω and slit area A.

In order to obtain spectral reflectance $\rho_u(\lambda)$, $L_u(\lambda)$ measurements are made of a 99-percent (near-Lambertian) horizontal diffuse reflector near the water surface. Values obtained are proportional to the spectrum being input to the water by the solar simulator. Reflectance is then computed by using the equation

$$\rho_u(\lambda) = \frac{|L_u(\lambda)|_{\text{Water mixture}}}{|L_u(\lambda)|_{\text{99-percent diffuse reflector}}} = \frac{L_u(\lambda)}{L_{so}(\lambda)} \tag{A5}$$

By adjusting the slit width, spectral resolution of the spectrometer may be changed. For the tests described herein, all laboratory measurements were made with a spectral resolution of 16 nm.

The instrument has been observed to experience daily variations in the calibration factor K which affects absolute accuracy. According to instrument specifications, absolute accuracy of the measurements is believed to be ±20 percent in the 400- to 600-nm range and ±12 percent in the 600- to 900-nm range. (A comparison of results from a number of laboratory tests at NASA tends to verify the manufacturer's specifications.) Included in the absolute error is a repeatability uncertainty of ±13 percent in the 400- to 600-nm range and ±3.5 percent in the 600- to 900-nm range. Discussions with the manufacturer indicate that these values are believed to be representative of 3σ error bands. Because of these absolute errors, spectral radiances from tests conducted on different days usually differ somewhat in magnitude. The overall shape of the relative spectrum over the wavelength range is consistent between tests conducted on different days.

Results from laboratory tests are always limited because the natural environment is not precisely duplicated. The effects of diffuse skylight, for instance, are not simulated in the laboratory used in this study. (The ratio of diffuse skylight to direct sunlight varies from day to day in the natural environment.) However, calculations with quasi-single scattering and multiple scattering optical models (ref. 11) have indicated less than 1-percent difference in reflectance between Sun-only and sky-only cases. For this reason, it was believed that reflectance spectra measured in the laboratory are generally characteristic of those in the natural environment for the same water mixture.

Measurements of upwelled radiance for clear waters in this laboratory are considered questionable. Data tabulated in reference 12 suggest that beam attenuation coefficient c should have a minimum value of 2.0 m^{-1} before bottom reflection can be ignored when water depth equals 3.0 m. Reference 13 examined the effects of solar spot size and concluded that c should have minimum values between 2.0 and 4.0 m^{-1} to eliminate losses in signal when spot diameter is 0.3 m. Data from this laboratory for turbid water with c greater than 4.0 m^{-1} should be considered valid.

REFERENCES

1. Moon, Parry: Proposed Standard Solar-Radiation Curves for Engineering Use. J. Franklin Inst., vol. 230, no. 5, Nov. 1940, pp. 583-617.

2. Witte, William G.; Usry, J. W.; Whitlock, Charles H.; and Gurganus, E. A.: Spectral Measurements of Ocean-Dumped Wastes Tested in the Marine Upwelled Spectral Signature Laboratory. NASA TP-1480, 1979.

3. Usry, J. W.; Whitlock, C. H.; Poole, L. R.; and Witte, W. G., Jr.: Laboratory Measurements of Selected Optical, Physical, Chemical, and Remote-Sensing Properties of Five Water Mixtures Containing Calvert Clay and a Non-Fluorescing Dye. NASA TM-81896, 1981.

4. Moore, Gerald K.: Satellite Surveillance of Physical Water-Quality Characteristics. Proceedings of the Twelfth International Symposium on Remote Sensing of Environment, Volume 1, Environmental Res. Inst. of Michigan, 1978, pp. 445-462.

5. Yarger, Harold L.; and McCauley, James R.: Quantitative Water Quality With LANDSAT and SKYLAB. NASA Earth Resources Survey Symposium. Volume I-A: Technical Session Presentations - Agriculture, Environment. NASA TM X-58168, 1975, pp. 347-370.

6. Rouse, L. J.; and Coleman, J. M.: Circulation Observations in the Louisiana Bight Using LANDSAT Imagery. Remote Sensing Environ., vol. 5, no. 1, 1976, pp. 55-66.

7. Munday, John C., Jr.; and Alföldi, Thomas T.: LANDSAT Test of Diffuse Reflectance Models for Aquatic Suspended Solids Measurement. Remote Sensing Environ., vol. 8, no. 2, May 1979, pp. 169-183.

8. Staff of the Color Measurement Lab., Massachusetts Inst. of Technology: Handbook of Colorimetry. Technology Press, 1936.

9. Schiebe, Frank R.; and Ritchie, Jerry C.: Color Measurements and Suspended Sediments in North Mississippi Reservoirs. Remote Sensing of Earth Resources, Volume IV, F. Shahrokhi, ed., Space Inst., Univ. of Tennessee, c.1975, pp. 543-553.

10. Stair, Ralph; Johnston, Russell, G.; and Halbach, E. W.: Standard of Spectral Radiance for the Region of 0.25 to 2.6 Microns. J. Res. Natl. Bur. Stand., vol. 64A, no. 4, July-Aug. 1960, pp. 291-296.

11. Gordon, H. R.; Brown, Otis B.; and Jacobs, Michael M.: Computed Relationships Between the Inherent and Apparent Optical Properties of a Flat Homogeneous Ocean. Appl. Opt., vol. 14, no. 2, Feb. 1975, pp. 417-427.

12. Whitlock, Charles H.: An Estimate of the Influence of Sediment Concentration and Type on Remote Sensing Penetration Depth for Various Coastal Waters. NASA TM X-73906, 1976.

13. Ghovanlou, A.: Radiative Transfer Model for Remote Sensing of Suspended Sediments in Water. NASA CR-145145, 1977.

TABLE I.- PHYSICAL AND CHEMICAL PROPERTIES OF WATER MIXTURES (MARCH 1980)

	Initial mixture	Mixture 1	Mixture 2	Mixture 3	Mixture 4	Mixture 5	Mixture 6
Total suspended solids-crucible (avg.[a]), ppm	1.0	4.5	67.8	123.3	183.5	225.2	326.7
Volatile suspended solids (avg.[a]), ppm	.7	1.5	10.2	23.3	31.0	41.1	51.1
Nonvolatile suspended solids (avg.[a]), ppm	.3	3.0	57.6	100.0	152.5	184.1	275.6
Iron, ppm	.05	.07	1.0	2.0	3.7	4.0	6.2
Copper, ppm	.45	.45	.45	.45	.46	.39	.48
Total organic carbon, ppm	<.1	.4	1.8	3.5	4.6	6.1	7.8
Particulate organic carbon, ppm	<.1	.1	.8	1.4	1.8	3.0	3.5
Dissolved organic carbon, ppm	<.1	.4	1.0	1.2	2.4	2.4	2.4
Inherent ICI chromaticity:							
Color, nm		562	578	580	582	582	583
Purity		0.0591	0.2699	0.3632	0.3976	0.4157	0.4165

[a]Average of 3 measurements.

TABLE II.- PHYSICAL AND CHEMICAL PROPERTIES OF WATER MIXTURES (DECEMBER 1980)

	Initial mixture	Mixture 1	Mixture 2	Mixture 3	Mixture 4	Mixture 5	Mixture 6	Mixture 7
Total suspended solids-crucible (avg.[a]), ppm	3.2	3.4	8.5	12.5	19.2	26.9	34.2	55.7
Total suspended solids-membrane (avg.[a]), ppm	1.3	5.6	11.1	18.7	26.2	34.1	46.5	70.5
Volatile suspended solids (avg.[a]), ppm		1.1	1.2	2.8	2.4	2.4	2.2	8.3
Nonvolatile suspended solids (avg.[a]), ppm		2.3	7.3	9.7	16.8	24.5	32.0	47.4
Iron, ppm	.05	.14	.23	.32	.40	.53	.71	1.1
Copper, ppm	.29	.29	.29	.49	.49	.62	.69	.66
Total organic carbon, ppm	<.2	<.2	<.2	1.6	1.4	2.1	2.6	2.7
Particulate organic carbon, ppm	.1	.1	.2	.5	.4	.6	.9	2.2
Dissolved organic carbon, ppm	<.2	<.2	<.2	.5	.7	1.8	1.2	1.4
Inherent ICI chromaticity:								
Color, nm		560	570	573	575	576	577	577
Purity		0.0396	0.0910	0.1426	0.1749	0.2216	0.2492	0.3054
Attenuation coefficient:								
At 550 nm		5.1	10.3	16.1	23.4	30.3	37.2	62.4
At 750 nm		6.3	9.4	13.2	18.2	22.1	29.6	43.0

[a]Average of 3 measurements.

TABLE II.- Concluded

	Mixture 8	Mixture 9	Mixture 10	Mixture 11	Mixture 12	Mixture 13	Mixture 14
Total suspended solids-crucible (avg.[a]), ppm	83.0	142.0	203.4	334.3	406.8	472.2	636.9
Total suspended solids-membrane (avg.[a]), ppm	93.4	155.2	207.0	313.7	430.2	570.1	691.2
Volatile suspended solids (avg.[a]), ppm	10.2	17.2	23.1	41.9	43.9	57.2	71.1
Nonvolatile suspended solids (avg.[a]), ppm	72.8	124.8	180.2	292.4	362.8	415.1	565.9
Iron, ppm	1.7	2.0	2.6	4.0	4.7	6.3	7.1
Copper, ppm	.67	.67	.63	.67	.68	.67	.67
Total organic carbon, ppm	2.0	3.4	4.8	8.0	5.1	8.4	11.6
Particulate organic carbon, ppm	1.1	2.2	2.4	3.8	2.2	2.8	3.5
Dissolved organic carbon, ppm	.3	.8	3.9	1.3	2.5	2.6	2.9
Inherent ICI chromaticity:							
Color, nm	579	582	582	582	582	582	582
Purity	0.3468	0.4311	0.4362	0.4586	0.4586	0.4614	0.4614
Attenuation coefficient:							
At 550 nm	76.2	139	208	314	389	446	464
At 750 nm	58.2	96.0	139	213	269	340	407

[a]Average of 3 measurements.

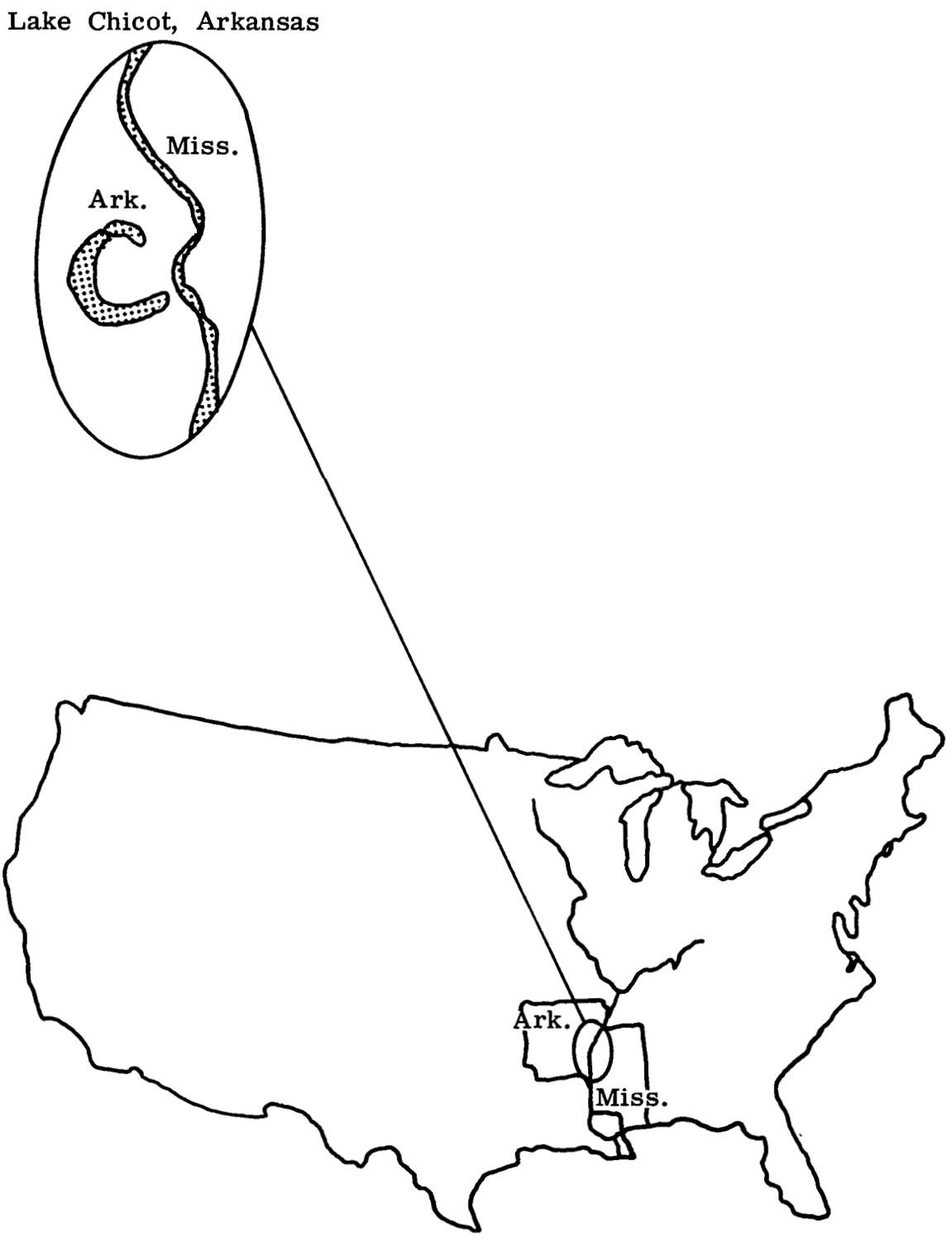

Figure 1.- Lake Chicot test site for AgRISTARS Conservation Assessment Task.

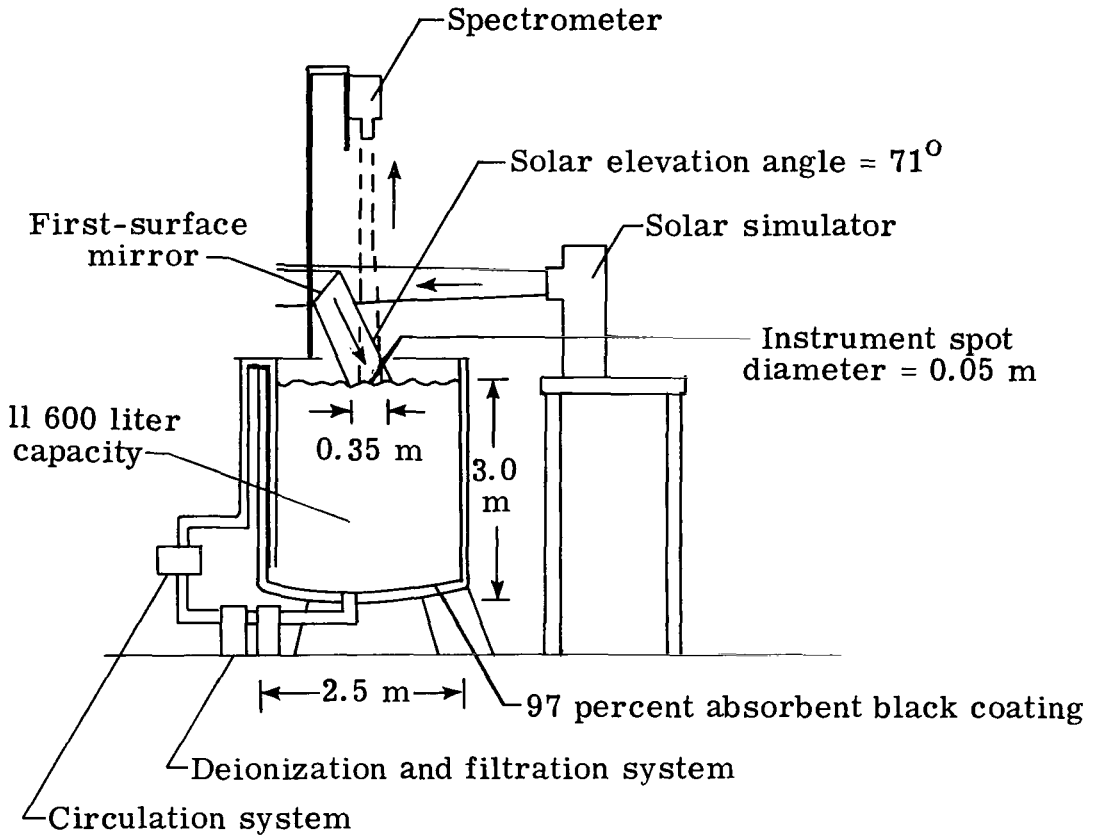

Figure 2.- Sketch of laboratory setup.

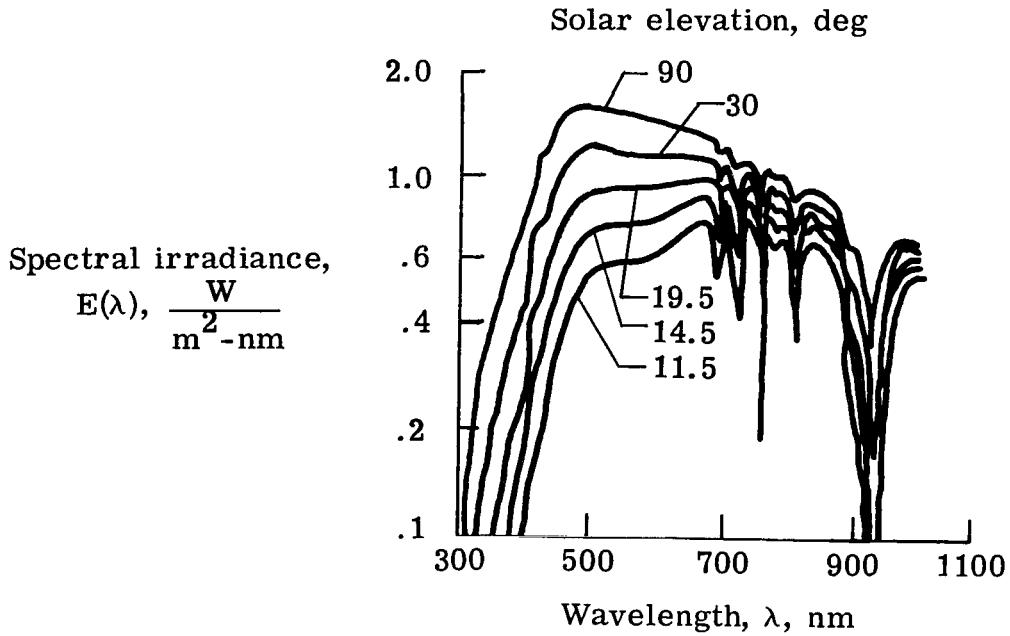

(a) Standard sea-level solar irradiance spectra (ref. 1).

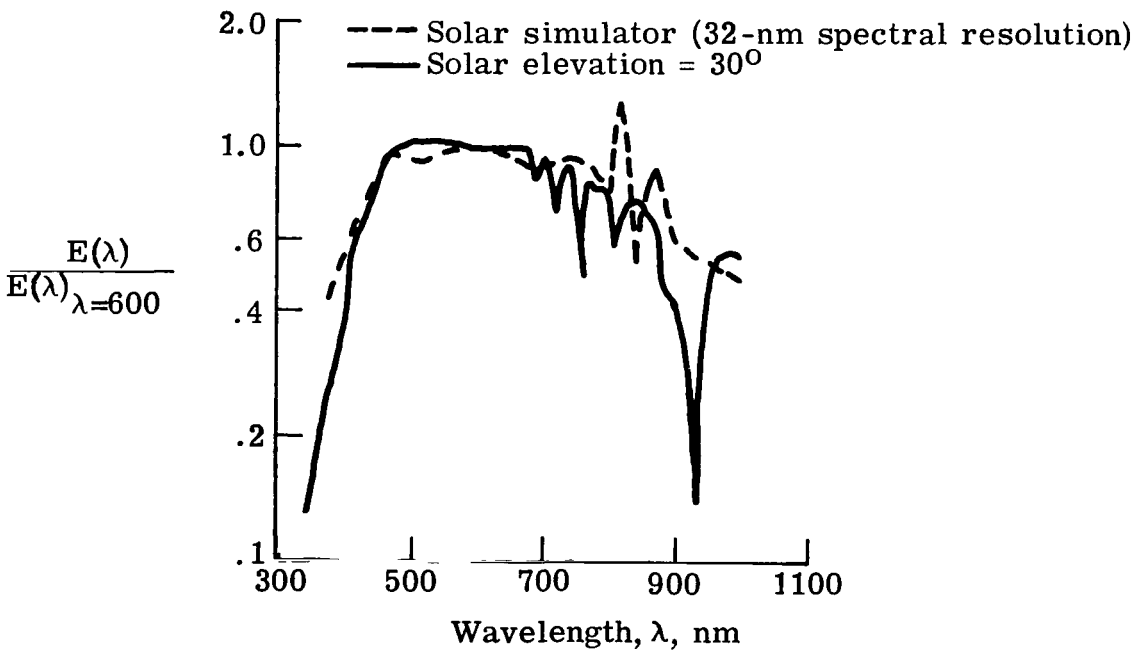

(b) Solar simulator and standard sea-level spectra.

Figure 3.- Standard sea-level solar irradiance spectra and comparison with solar simulator data.

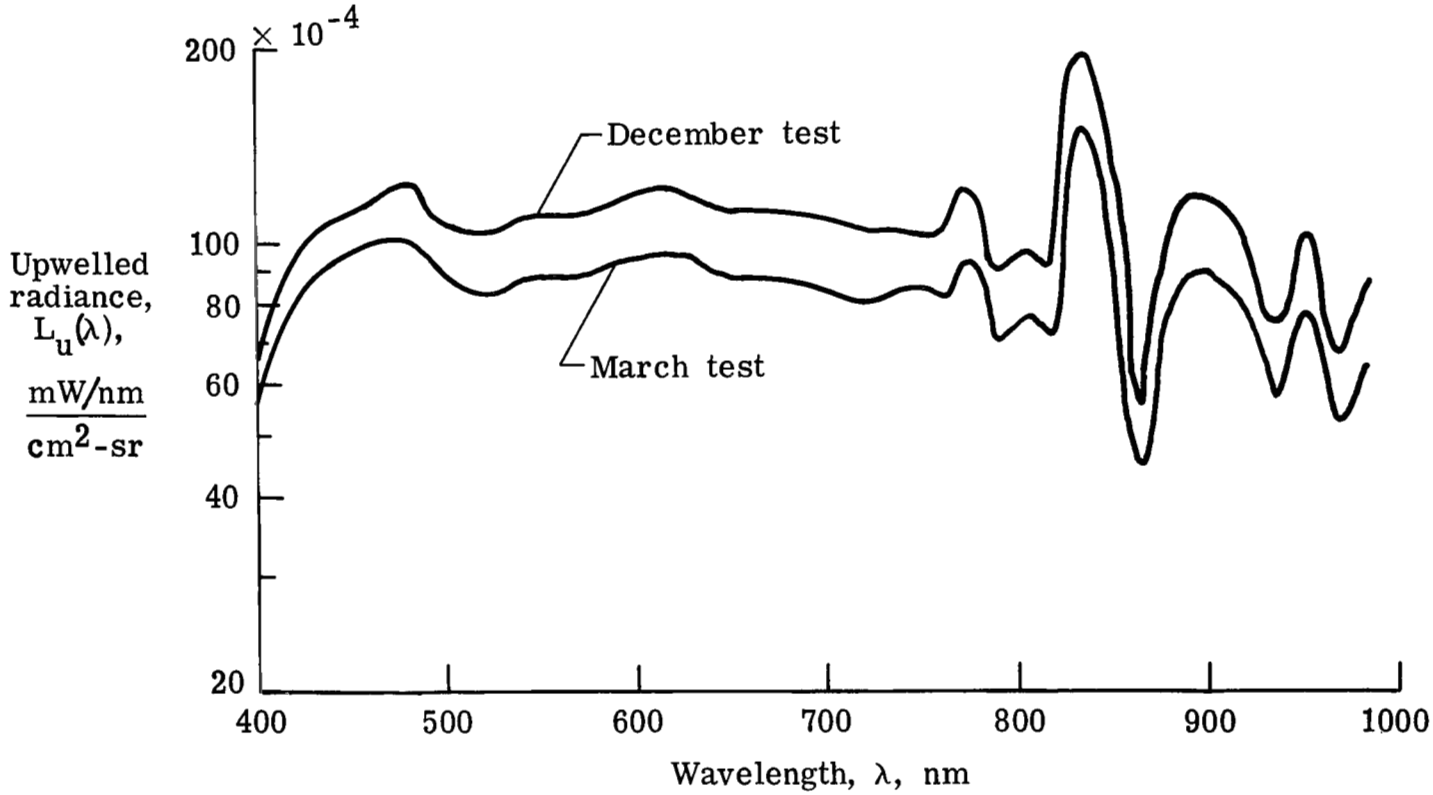

Figure 4.- Upwelled radiance of white card.

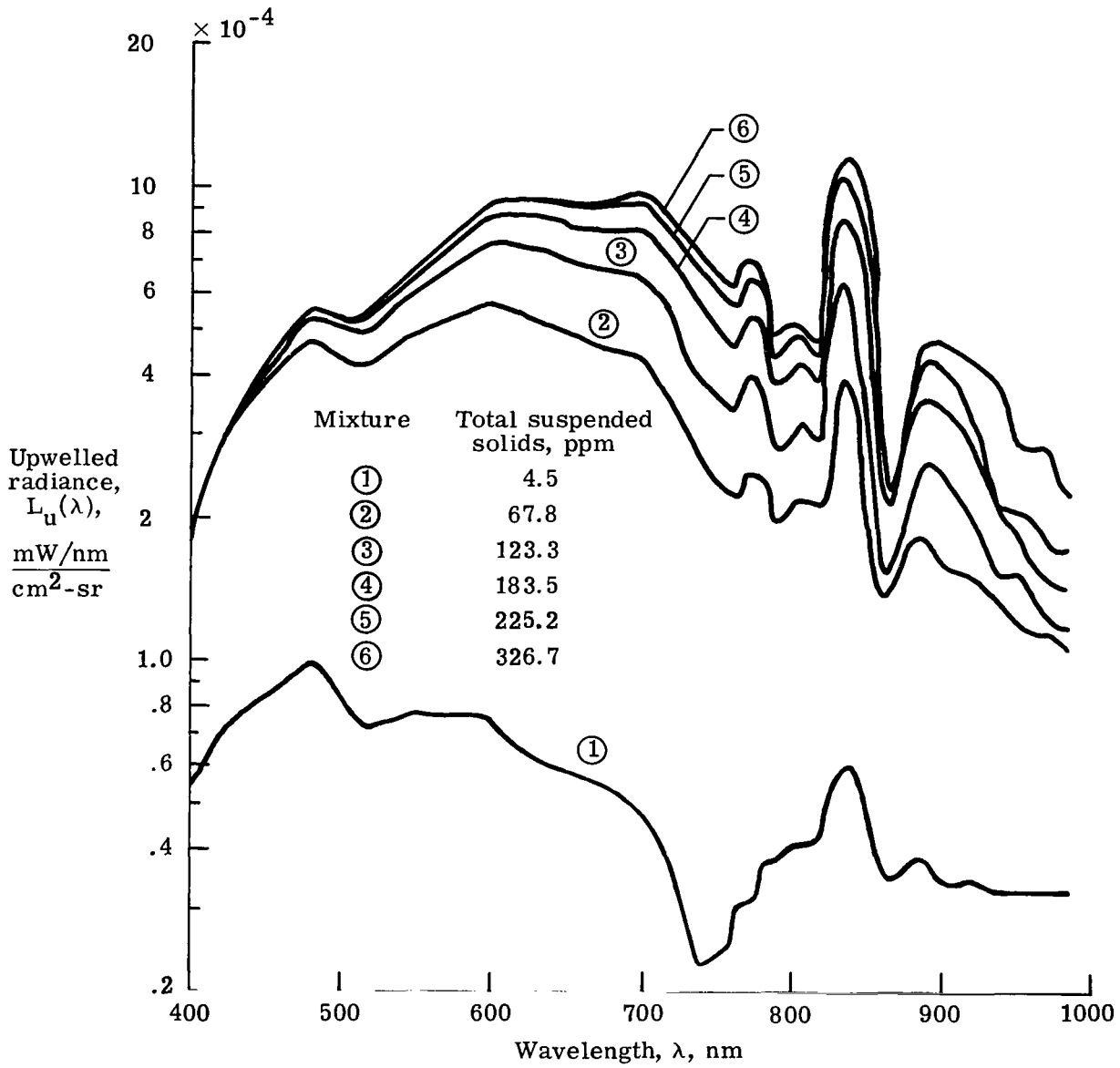

(a) March test.

Figure 5.- Upwelled radiance for the mixtures.

Mixture	Total suspended solids, ppm	Mixture	Total suspended solids, ppm
①	3.4	⑧	83.0
②	8.5	⑨	142.0
③	12.5	⑩	203.4
④	19.2	⑪	334.3
⑤	26.9	⑫	406.8
⑥	34.2	⑬	472.2
⑦	55.7	⑭	636.9

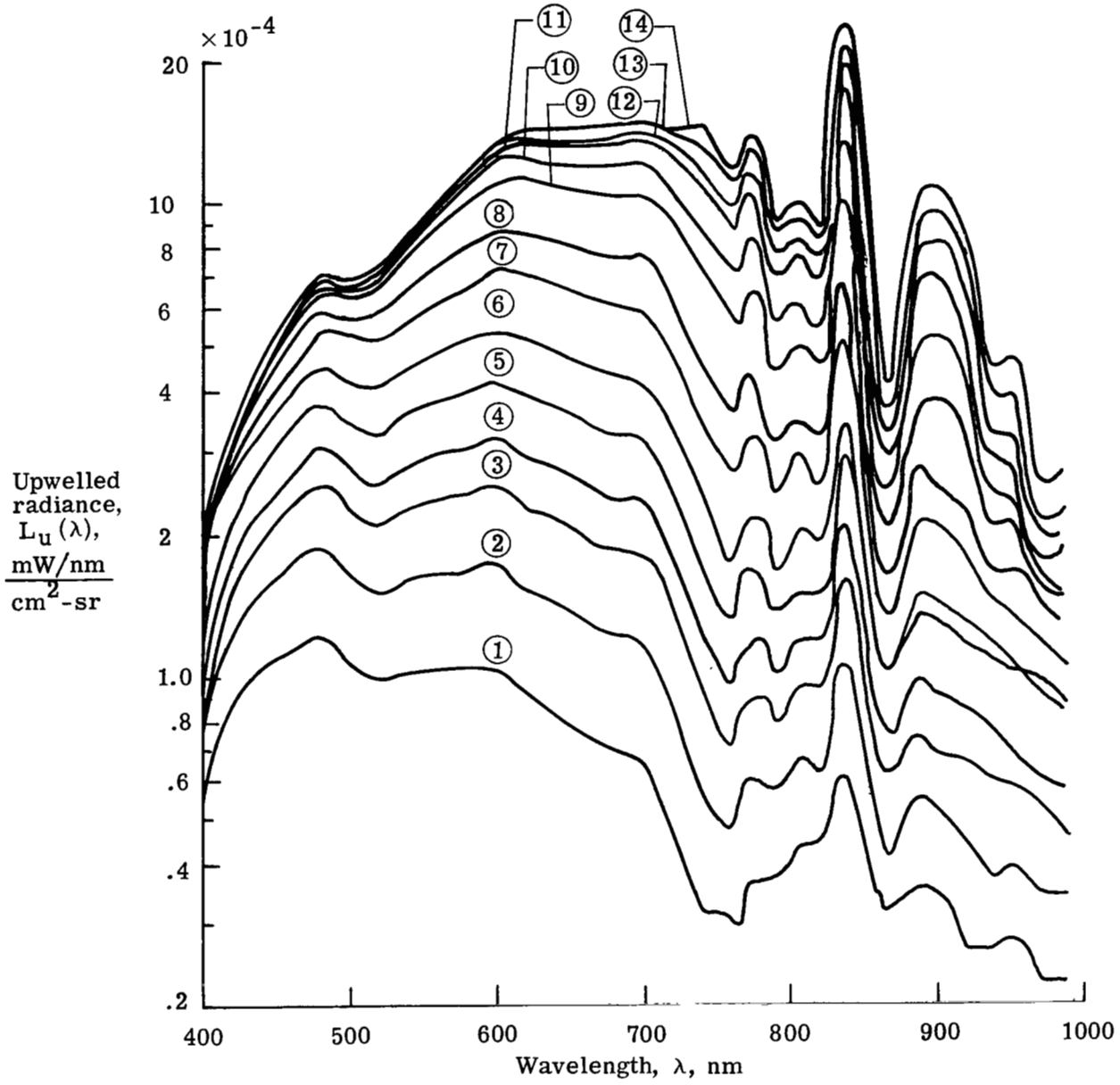

(b) December test.

Figure 5.- Concluded.

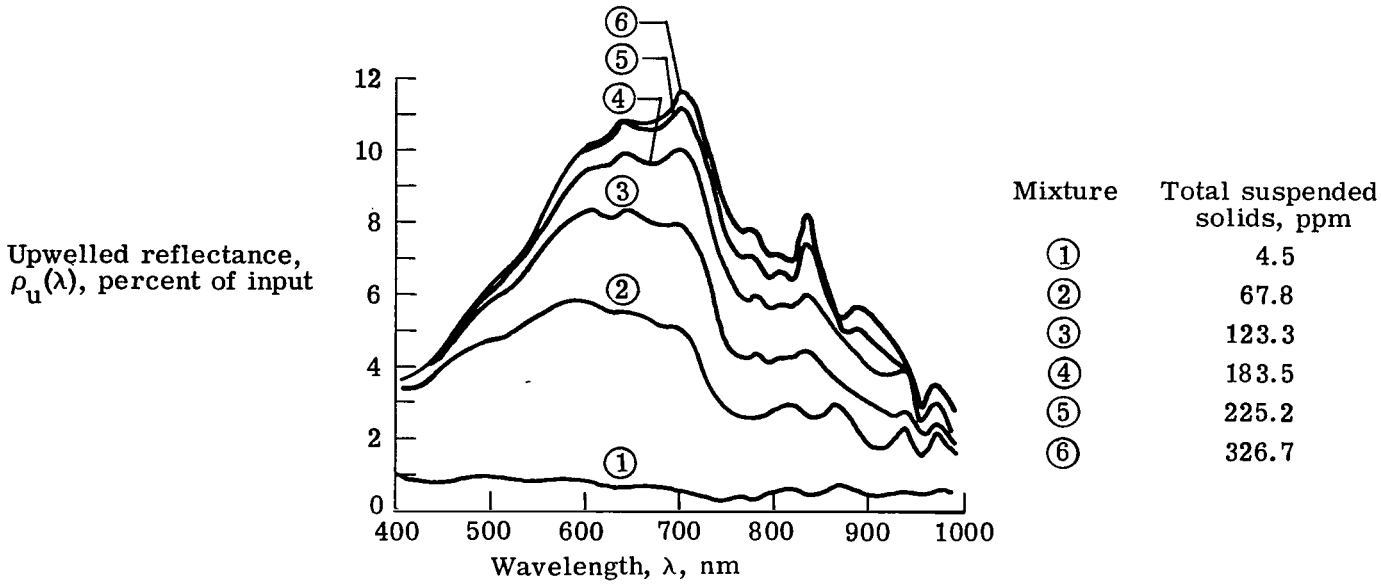

(a) March test.

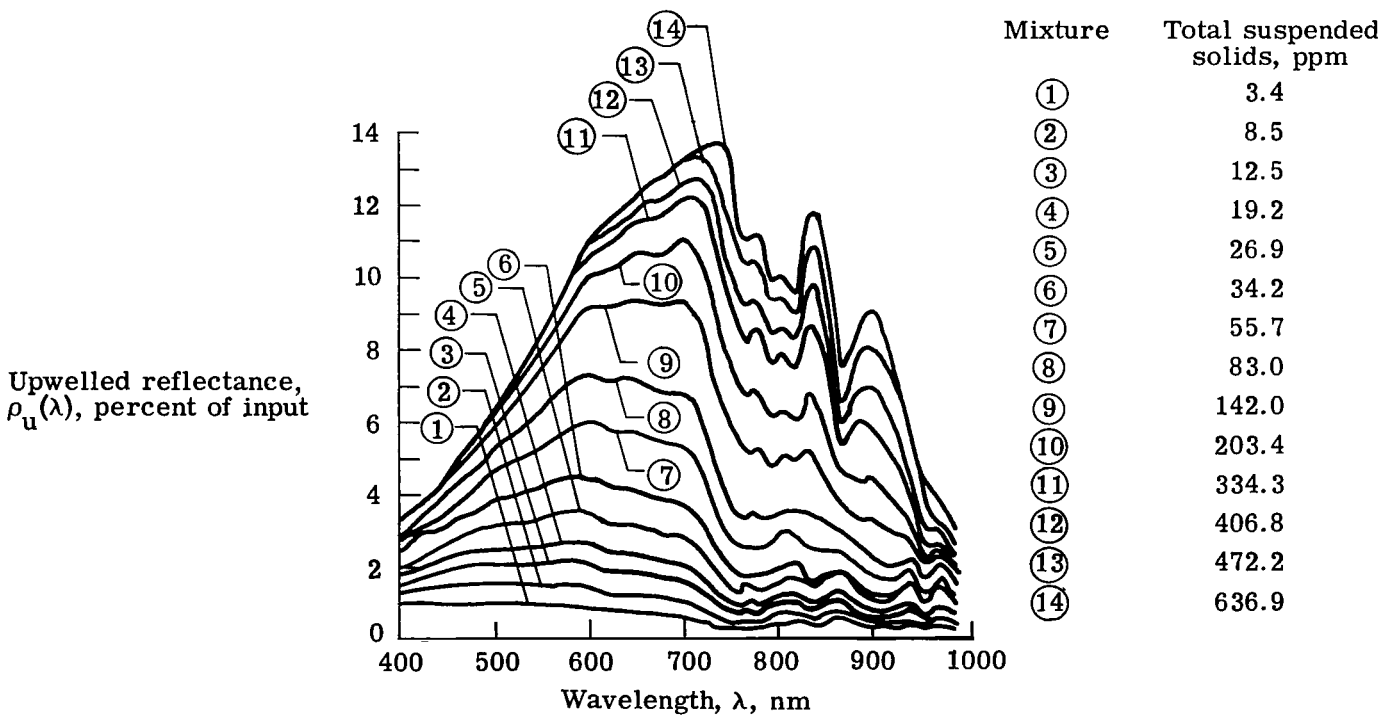

(b) December test.

Figure 6.- Upwelled reflectance for the mixtures.

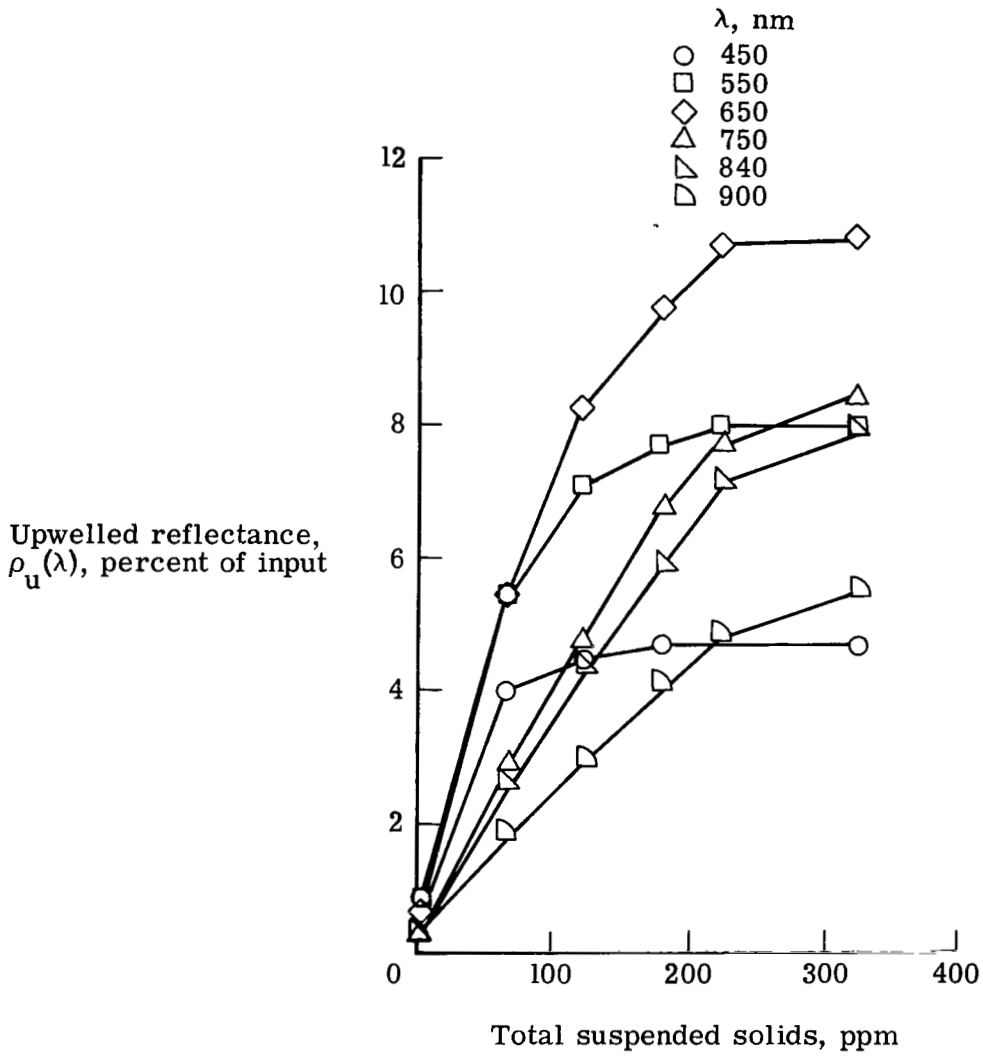

(a) March test.

Figure 7.- Upwelled reflectance versus total suspended solids.

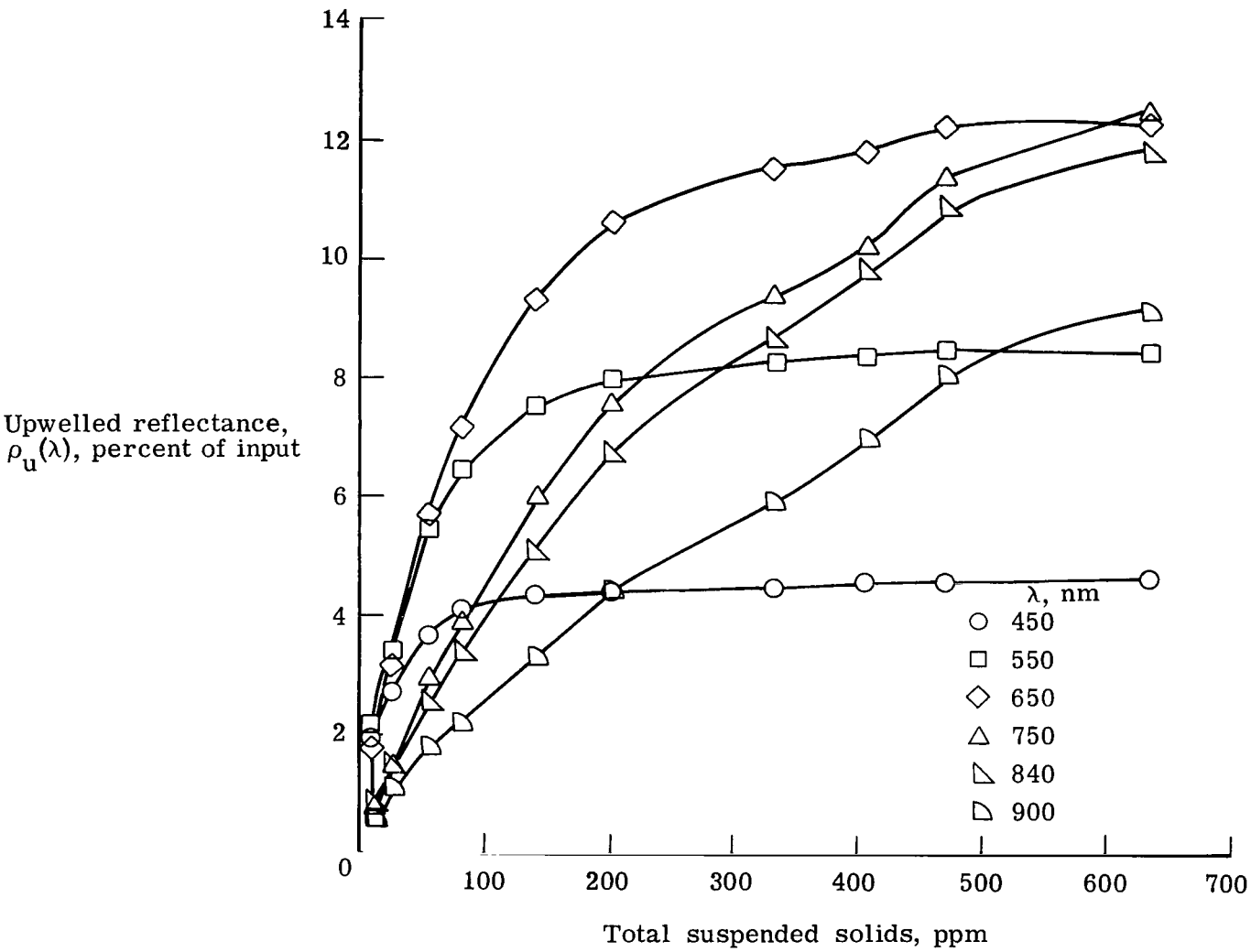

(b) December test.

Figure 7.- Concluded.

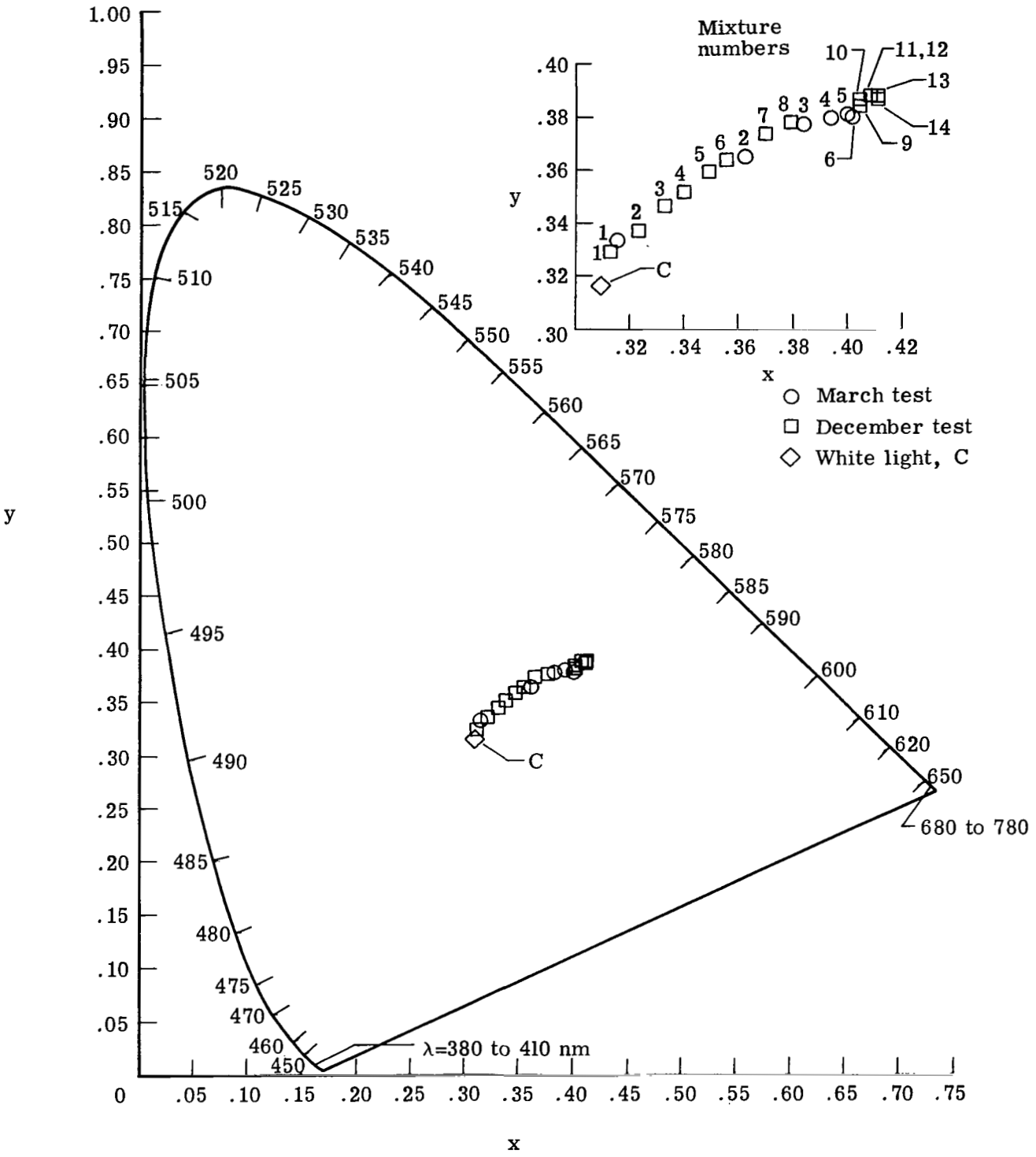

Figure 8.- ICI chromaticity.

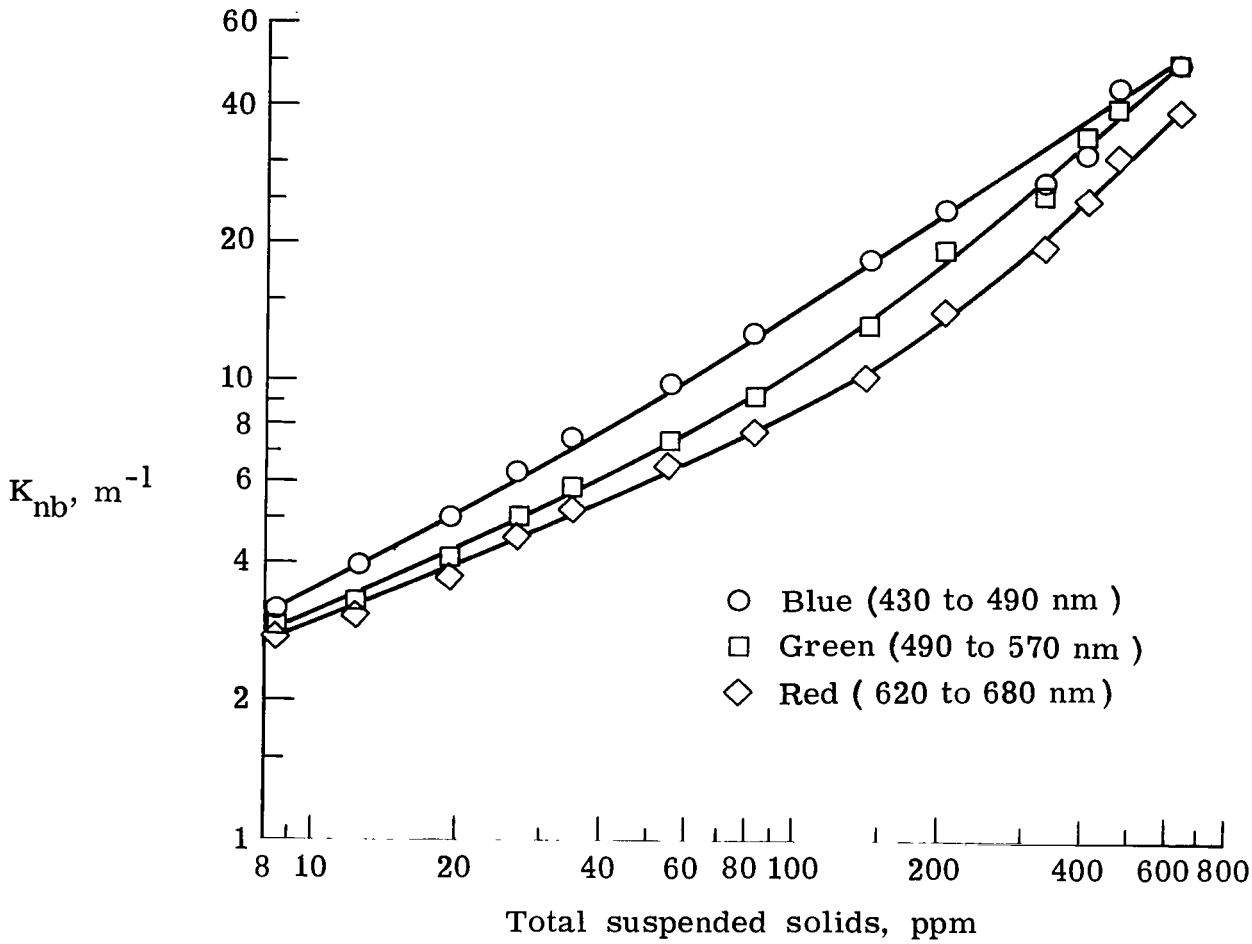

(a) Narrow-band data (December test).

Figure 9.- Diffuse attenuation coefficient versus total suspended solids.

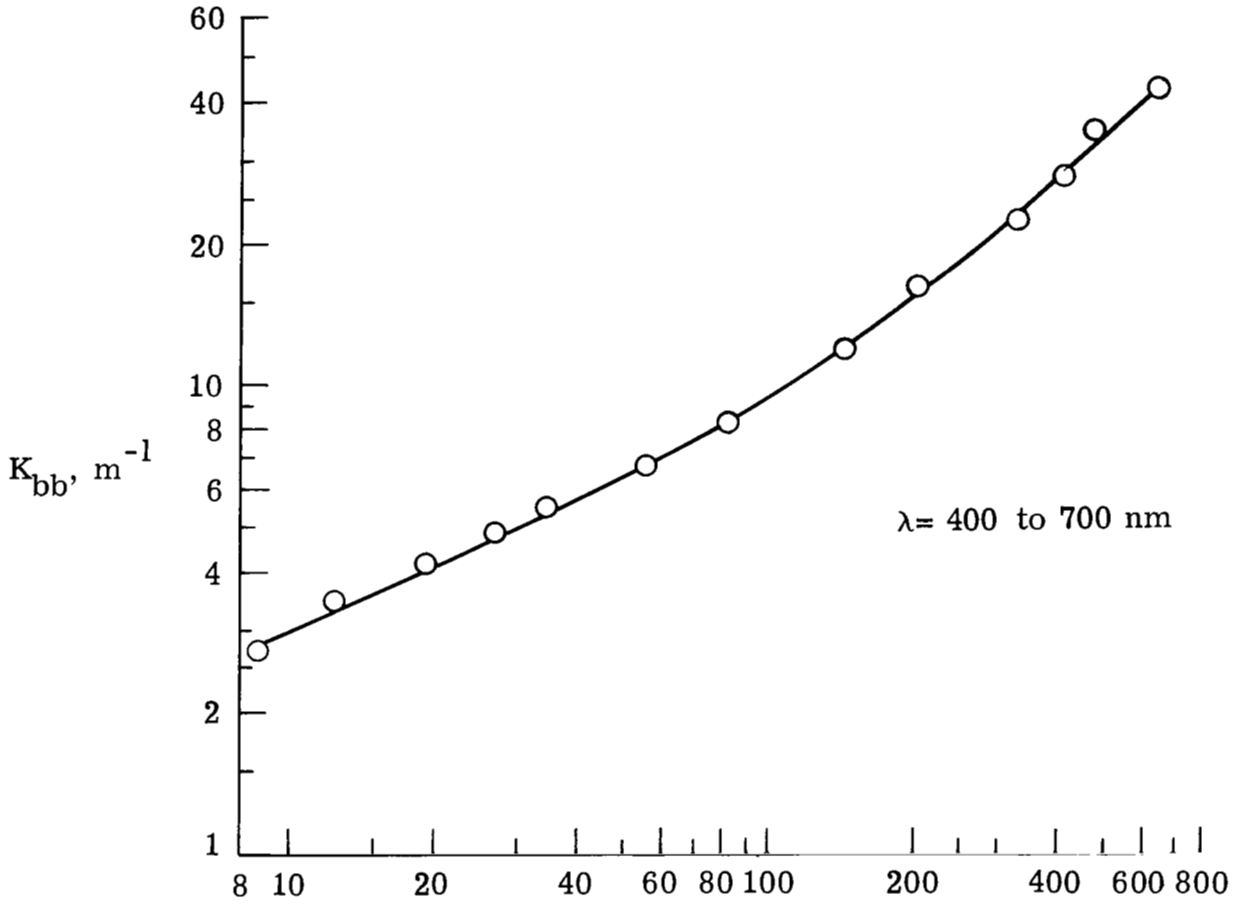

(b) Broad-band data (December test).

Figure 9.- Concluded.

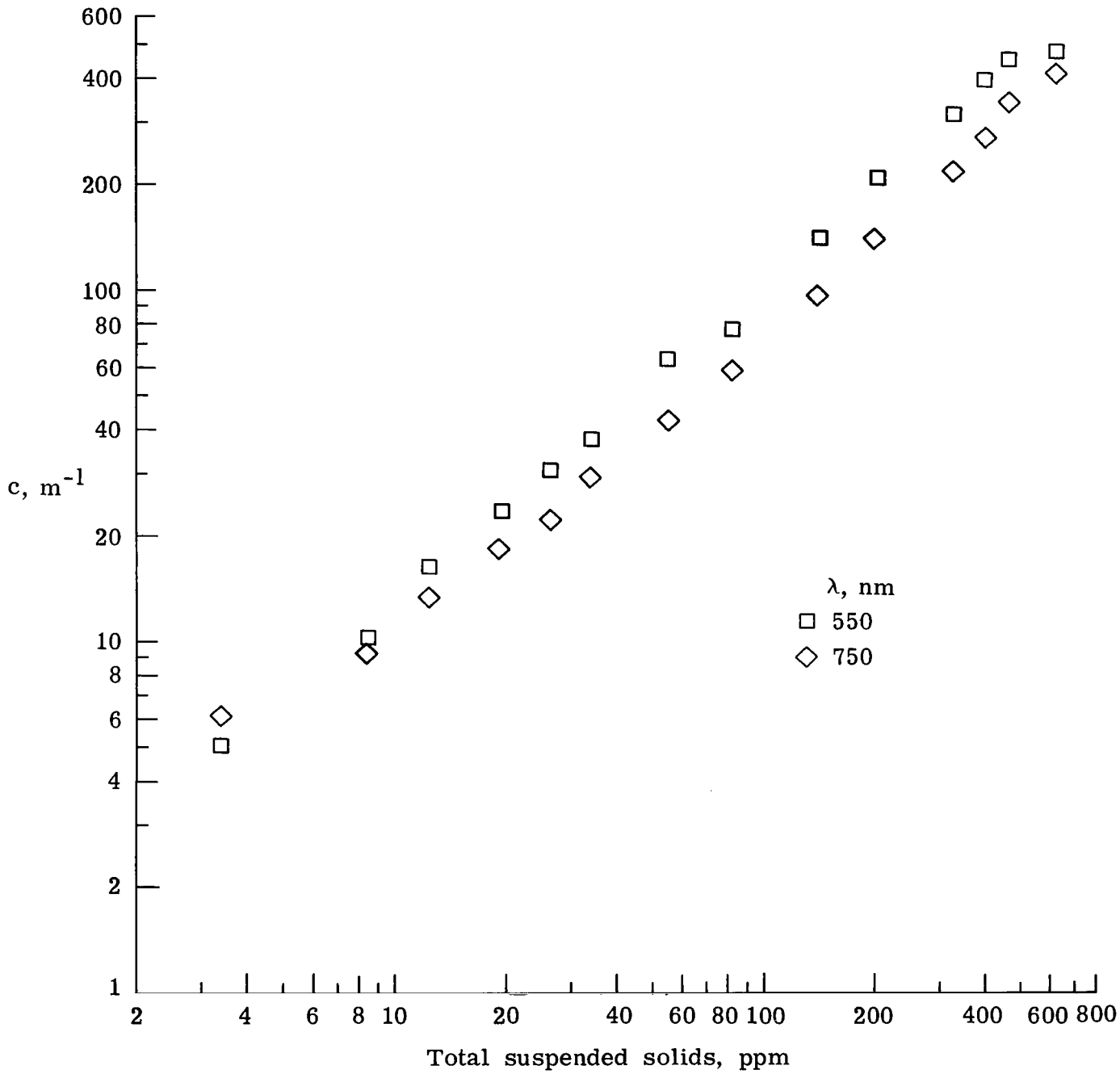

Figure 10.- Beam attenuation coefficient versus total suspended solids (December test).

1. Report No.	2. Government Accession No.	3. Recipient's Catalog No.
NASA TP-1941		

4. Title and Subtitle	5. Report Date
LABORATORY MEASUREMENTS OF PHYSICAL, CHEMICAL, AND OPTICAL CHARACTERISTICS OF LAKE CHICOT SEDIMENT WATERS	December 1981
	6. Performing Organization Code: 691-09-02-01
7. Author(s): William G. Witte, Charles H. Whitlock, J. W. Usry, W. Douglas Morris, and E. A. Gurganus	8. Performing Organization Report No.: L-14714
	10. Work Unit No.
9. Performing Organization Name and Address: NASA Langley Research Center, Hampton, VA 23665	11. Contract or Grant No.
	13. Type of Report and Period Covered: Technical Paper
12. Sponsoring Agency Name and Address: National Aeronautics and Space Administration, Washington, DC 20546	14. Sponsoring Agency Code

15. Supplementary Notes

16. Abstract

Reflectance, chromaticity, diffuse attenuation, beam attenuation, and several other physical and chemical properties are measured for various water mixtures of bottom sediment from Lake Chicot, Arkansas. Mixture concentrations range from 5 ppm to 700 ppm by weight of total suspended solids in filtered deionized tap water. Upwelled reflectance is observed to be a nonlinear function of total suspended solids with the degree of nonlinearity a strong function of remote-sensing wavelengths. Near-infrared wavelengths appear useful for monitoring highly turbid waters with sediment concentrations above 100 ppm. Chromaticity characteristics do not appear useful for monitoring sediment concentrations above 100 ppm. At both visible and near-infrared wavelengths, beam attenuation correlates well with total suspended solids ranging over two orders of magnitude.

17. Key Words (Suggested by Author(s))	18. Distribution Statement
Remote sensing Spectral signature Laboratory measurements Marine sediments	Unclassified - Unlimited Subject Category 43

19. Security Classif. (of this report)	20. Security Classif. (of this page)	21. No. of Pages	22. Price
Unclassified	Unclassified	28	A03

For sale by the National Technical Information Service, Springfield, Virginia 22161

NASA-Langley, 1981

National Aeronautics and
Space Administration

Washington, D.C.
20546

Official Business
Penalty for Private Use, $300

THIRD-CLASS BULK RATE

Postage and Fees Paid
National Aeronautics and
Space Administration
NASA-451

NASA

POSTMASTER: If Undeliverable (Section 158 Postal Manual) Do Not Return